

Na₉K₁₆Tl₁₈Cd₃: A Novel Phase Containing Tl₈Cd₃¹⁰⁻ and Tl₅⁷⁻ Clusters¹

DaPing Huang and John D. Corbett*

Ames Laboratory—DOE and Department of Chemistry, Iowa State University, Ames, Iowa 50011

Received July 7, 1998

Reaction of the elements in tantalum containers at 450 °C followed by slow cooling yields the title phase, which crystallizes in the hexagonal space group *P6₃/mmc* (No. 194), *Z* = 2, *a* = 11.136(6) Å, *c* = 29.352(7) Å. The compound contains separate layers of Tl₈Cd₃¹⁰⁻ and Tl₅⁷⁻ clusters separated by Na⁺ and K⁺ cations, viz., (Na⁺)₉(K⁺)₁₆(Tl₅⁷⁻)₂(Tl₈Cd₃¹⁰⁻)e⁻. The new Tl₈Cd₃¹⁰⁻ is a pentacapped trigonal prism (*D_{3h}*), isosteric and isoelectronic with Tl₁₁⁷⁻, with Cd substituted in the waist-capping positions, the vertexes with the least negative Mulliken charge in the parent cluster. The compound is semiconducting and Curie–Weiss paramagnetic (–1.50 μ_B), these evidently reflecting the extra electron trapped in some alkali-metal-bordered cavity. Some energetics of the atom substitution reaction are considered.

Introduction

Alkali-metal–triel (Tr) systems feature an abundance of phases containing isolated cluster or network polyanions, especially for Tr = Ga, In, and Tl.^{2,3} Among these, gallium forms mostly network structures and only a few with isolated clusters,⁴ while thallium is the richest in individual clusters, e.g., Tl₄⁸⁻,⁵ Tl₅⁷⁻,⁶ Tl₆⁶⁻,⁷ Tl₉⁹⁻,⁶ Tl₁₁⁷⁻,^{8,9} and Tl₁₃¹⁰⁻,^{11–10} as well as examples with centered heteroatoms such as Tl₁₂Na¹³⁻,¹¹ Tl₁₂Mg¹²⁻,¹² and Tl₁₀Zn⁸⁻.¹³ The first substituted cluster Tl₉Au₂⁹⁻ was discovered in K₁₈Tl₂₀Au₃, a distorted version of the pentacapped trigonal prismatic Tl₁₁⁷⁻ in which axial substitution has led to a strong compression and the formation of a transannular Au–Au bond.¹⁴ Most of these clusters are closed-shell and obey (modified) Wade's rules,^{3,15} although the A₈Tl₁₁ phases (A = K–Cs)⁸ and the foregoing gold phase each have one extra cation and a delocalized electron per formula unit, evidently for packing reasons, while Na₄A₆Tl₁₃ (A = K, Rb, Cs) has a localized hole in the Tl₁₃¹⁰⁻ cluster.¹⁰

Our continuing explorations of the substitution of earlier metals into triel clusters have now revealed the unusual Tl₈Cd₃¹⁰⁻ derivative of Tl₁₁⁷⁻ in the title compound Na₉K₁₆Tl₁₈Cd₃. As has been seen many times before, the use of mixed

alkali metals often affords a new packing arrangement that allows the isolation of new cluster units.³ We will later report on substitution in the opposite direction that produces the Tl₉Cd₂⁷⁻ analogue of Tl₉Au₂⁹⁻.¹⁶

Experimental Section

Syntheses. The general techniques of synthesis in welded Ta tubing, glovebox use, and Guinier powder diffraction have been described elsewhere.^{6–9} The title compound was synthesized by reaction of the constituent elements, the surfaces of the Na (99.9% Alpha), K (99.9% Baker), Tl, and Cd (99.998%, Johnson-Matthey) being removed with a scalpel beforehand. The phase was first seen after a reaction with stoichiometry Na₂K₂Tl₂Cd had been run at 400 °C for 4 days followed by cooling to room temperature at 1 °C/h. The product consisted of three phases: 70% of the title phase (as thin truncated hexagonal bipyramids), 15% NaCd₂,¹⁷ and a liquid alloy of mainly the alkali metals. Both kinds of crystals had evidently grown from the liquid mixture. Some crystals of the title phase were cleaned in grease and sealed in capillaries for crystallographic measurements.

A sample with the stoichiometry indicated by the structural solution (below) was later reacted at 450 °C for 3 days and then cooled as before. This gave a brittle, shiny crystalline product that was single phase Na₉K₁₆Tl₁₈Cd₃ according to its Guinier powder pattern. This product was used for electrical and magnetic property measurements. Most of the crystals were large (about 4 × 4 × 4 mm). The crystals were very sensitive to traces of moisture, turning gray in half an hour in the glovebox. The elemental composition of crystals from the first reaction was determined through energy-dispersive X-ray spectroscopy (EDS) on JEOL 840A SEM with an IXRF system X-ray analyzer and a Kevex Quantum light element detector. Crystals with freshly cut faces were analyzed with a beam of 20 kV and 0.3 nA for count rates of about 2500 s⁻¹. The EDS examination resulted in a Na/K/Tl/Cd composition of 21:34:38:7 at. %, or 9.9:16.1:18:3.3, close to the crystal structure result Na₉K₁₆Tl₁₈Cd₃. Measurements on crystals from the second reaction gave similar results within 3–5%.

Property Measurements. Magnetic susceptibility measurements were made on 83.4 mg of Na₉K₁₆Tl₁₈Cd₃ at the field of 3 T over the range of 6–300 K with the aid of a Quantum Design MPMS SQUID magnetometer. The sample under He gas was held between two fused silica rods that were in turn fixed inside a closely fitting silica tube that was sealed at both ends. The raw magnetic data were corrected

- (1) This research was supported by the Office of the Basic Energy Sciences, Materials Sciences Division, U.S. Department of Energy. The Ames Laboratory is operated by DOE by Iowa State University under Contract No. W-7405-Eng-82.
- (2) Belin, C.; Tillard-Charbonnel, M. *Prog. Solid State Chem.* **1993**, *22*, 59.
- (3) Corbett, J. D. In *Chemistry, Structure and Bonding of Zintl Phases and Ions*; Kauzlarich, S., Ed.; VCH Publishers: New York, 1996; Chapter 3.
- (4) Henning, R. W.; Corbett, J. D. *Inorg. Chem.* **1997**, *36*, 6049.
- (5) Smith, J. F.; Hansen, D. A. *Acta Crystallogr.* **1967**, *22*, 836.
- (6) Dong, Z.-C.; Corbett, J. D. *J. Am. Chem. Soc.* **1994**, *116*, 3429.
- (7) Dong, Z.-C.; Corbett, J. D. *Inorg. Chem.* **1996**, *35*, 2301.
- (8) Dong, Z.-C.; Corbett, J. D. *J. Cluster Sci.* **1995**, *6*, 187.
- (9) Dong, Z.-C.; Corbett, J. D. *Inorg. Chem.* **1996**, *35*, 1444.
- (10) Dong, Z.-C.; Corbett, J. D. *J. Am. Chem. Soc.* **1995**, *117*, 6447.
- (11) Dong, Z.-C.; Corbett, J. D. *Inorg. Chem.* **1995**, *34*, 5709.
- (12) Dong, Z.-C.; Corbett, J. D. *Angew. Chem., Int. Ed. Engl.* **1996**, *35*, 1006.
- (13) Dong, Z.-C.; Henning, R. W.; Corbett, J. D. *Inorg. Chem.* **1997**, *36*, 3559.
- (14) Dong, Z.-C.; Corbett, J. D. *Inorg. Chem.* **1995**, *34*, 5042.
- (15) Corbett, J. D. *Struct. Bonding* **1997**, *87*, 157.

(16) Huang, D.-P.; Corbett, J. D., to be submitted.

(17) Yang, Q.-B.; Andersson, S.; Stenberg, L. *Acta Crystallogr.* **1987**, *43B*, 14.

for the susceptibilities of the container and the diamagnetism of the cores. The electrical resistivities of the phase were measured by an electrodeless Q method on a 150 mg sample sieved to a 250–425 μm powder and diluted with Al₂O₃. The measurements were made at 34 MHz over 100–290 K.

EHMO Calculations. The EHMO program package from the R. Hoffmann group was used for bonding and charge distribution calculations. The ξ values employed were taken from Alvarez¹⁸ while the H_{ii} values came from density functional theory (Cd 5p, -4.933; 5s, -9.253; Tl, 6p, -5.715; 6s, -11.525 eV).¹⁹

Structure Determination. The structure was actually solved and refined with data from three different crystals. Thin truncated hexagonal bipyramidal crystals were chosen on the basis of Polaroid Laue photos taken on the Rigaku AFC6R diffractometer with graphite-monochromated Mo Kα radiation. Least-squares refinements for each of 25 tuned reflections from a random search in the range of 14 to 20° yielded an orientation matrix and the hexagonal cell constants near $a = 11.179(7)$ Å, $c = 29.424(8)$ Å. The axial repeat lengths were also checked by Polaroid photographs on the diffractometer. One octant of data was collected at 23 °C in the 2θ range of 3 to 55° using the ω scan technique and a scan speed of 16°/min with a scan width of 1.3 + 0.34 tan θ. Weak reflections ($I < 10σ(I)$) were recounted to ensure good counting statistics. The intensities of three representative reflections measured after every 150 reflections remained constant throughout data collection, indicating crystal and electronic stability.

Of the 2881 reflections measured for the best result, 1561 were unique and 432 were observed ($I > 3σ_I$). The raw data were corrected with the aid of ψ scans of three strong reflections. The Laue class was determined to be $6/mmm$ and the absence condition $hhl: l...2n$ indicated three possible space groups, $P6_3mc$ (No. 186), $P6_2c$ (No. 190) and $P6_3/mmc$ (No. 194), and the high-symmetry $P6_3mc$ yielded initial solutions of high merit.

The structure was solved via direct methods with SHELXS86.²⁰ All of the Tl and Cd atoms were correctly identified in the initial output. Subsequent refinements using the TEXSAN²¹ software package allowed the location of all cations and gave $R(F)/R_w = 0.119/0.115$ (isotropic). DIFABS²² was then used for an improved absorption correction for the thin crystal (5:1 aspect ratio; $μ = 483.8$ cm⁻¹, transmission range = 0.42–1.0). This resulted in general 2- to 3-fold decreases in coordinate errors, 2–28% reductions of heavy atom B parameters and -45 to (in one case) +50% changes in cation B values. The data then averaged with $R_{int} = 16%$ for $I > 3σ_I$ and gave a significantly better isotropic refinement, $R/R_w = 5.4/5.6%$. The final cycle of full-matrix least-squares anisotropic refinement converged at $R(F)/R_w = 2.6/2.6%$ (432 data, 55 variables). The maximum and minimum peaks in the final difference Fourier map were 2.00 and -2.09 e/Å³, 1.8 and 1.3 Å from Tl1, respectively. Although B_{eq} of Cd seemed a little small, refinement of its occupancy (mixed with Tl) at the isotropic stage after absorption corrections yielded a value of 0.920(16) ($B(Cd) = 1.0(1)$), that is, slightly low but only at the 5σ level. This was not considered significant. The calculated powder pattern agrees very well with that measured.

Some details of data collection and refinement are listed in Table 1, the atomic positional and isotropic displacement parameters are in Table 2, and the important interatomic distances appear in Table 3. More details as well as the anisotropic parameters are in the Supporting Information. These and the structure factor data are also available from J. D. C.

Results and Discussion

Structure. Reasonable oxidation state assignments (below) lead to a $[(Na^+)_{16}(K^+)_{16}(Tl_5^{7-})_2(Tl_8Cd_3^{10-})e^-]$ representation for the new Na₉K₁₆Tl₁₈Cd₃. The two naked anionic clusters

Table 1. Some Data Collection and Refinement Parameters for Na₉K₁₆Tl₁₈Cd₃

formula wt	4848.4
crystal system	hexagonal
space group, Z	$P6_3/mmc$ (No. 194), 2
lattice Constants (Å) ^a	
<i>a</i>	11.136(6)
<i>c</i>	29.352(7)
volume (Å ³)	3153(2)
d_c (g/cm ³)	5.106
$μ$, cm ⁻¹ (Mo Kα)	483.76
R/R_w (%) ^b	2.6/2.6

^a Guinier powder pattern data, $λ = 1.540562$ Å, 23 °C. ^b $R = \sum ||F_o| - |F_c|| / \sum |F_o|$; $R_w = [\sum w(|F_o| - |F_c|)^2 / \sum w(F_o)^2]^{1/2}$; $w = σ_F^{-2}$.

Table 2. Atomic Position and Isotropic-Equivalent Thermal Factors for Na₉K₁₆Tl₁₈Cd₃

atom	<i>x</i>	<i>y</i>	<i>z</i>	B_{eq}^a
Tl1	0.2339(1)	2 <i>x</i>	0.44557(6)	1.1(1)
Tl2	¹ / ₃	² / ₃	0.5303(1)	1.14(8)
Tl3	¹ / ₃	² / ₃	0.3602(1)	1.32(9)
Tl4	0	0	0.6587(1)	1.31(8)
Tl5	0.1586(1)	2 <i>x</i>	0.69658(5)	1.70(8)
Cd1	0.1042(2)	2 <i>x</i>	¹ / ₄	0.7(3)
K1	0.1290(5)	2 <i>x</i>	0.5589(4)	2.6(5)
K2	0.4556(8)	2 <i>x</i>	¹ / ₄	2(1)
K3	0.4626(5)	2 <i>x</i>	0.6247(4)	2.6(7)
K4	¹ / ₃	² / ₃	³ / ₄	3(1)
Na1	0.163(1)	2 <i>x</i>	0.3473(6)	3(1)
Na2	¹ / ₂	0	¹ / ₂	2(1)

^a $B_{eq} = (8π^2/3) \sum_i \sum_j U_{ij} a_i^* a_j^* \bar{a}_i \bar{a}_j$.

Tl₈Cd₃¹⁰⁻ and Tl₅⁷⁻ are naturally of most interest. Two views of the cell are shown in Figures 1 and 2. The novel Tl₈Cd₃¹⁰⁻ clusters lie on mirror planes at $z = 1/4$, as well as on 3-fold (and 6₃) axes along 0, 0, z . The Tl₅⁷⁻ anions are centered at a , b , 0.55 and b , a , 0.45, while the cations separate the anionic clusters. The novel Tl₈Cd₃¹⁰⁻ cluster, shown in detail in Figure 3a, consists of a pentacapped trigonal prism that has been compressed along 3-fold axis and expanded laterally. It, like its counterpart Tl₁₁⁷⁻ in Rb₁₅Tl₁₇,⁹ possesses D_{3h} symmetry while these anions in the A₈Tl₁₁ family (A = K–Cs) deviate only slightly to D_3 .⁸ The cadmium substitutes in the three waist-capping sites, and this leads to a compression of the trigonal prism by -0.08 Å and a small lateral expansion of 0.16 Å as measured by $d(Tl5-Tl5)$. Opposite changes occur for the axial Tl4, a 0.09 Å reduction for $d(Tl4-Cd)$ and a 0.11 Å expansion in $d(Tl4-Tl5)$ relative to that in Tl₁₁⁷⁻. The distances between the trigonal prismatic atoms and the waist caps (Tl5–Cd) increase only very slightly, -0.01 Å. Expectations for Tl → Cd distance changes are difficult to assess. Although the 12-coordinate and single bond metallic radii of Cd (1.508, 1.382 Å)²³ are 0.087 and 0.055 Å less than for Tl, respectively, the average bond distance in Tl₈Cd₃¹⁰⁻, 3.22 Å, in fact compares very well with 3.22 Å for Tl₁₁⁷⁻ in Rb₁₅Tl₁₇ and 3.20 Å in A₈-Tl₁₁. (The Cd radius according to the length of its transannular and perhaps strained Cd–Cd bond in Tl₉Cd₂¹¹⁻¹⁶ is larger, 1.58 Å.) Cluster distortions are evidently effective in giving cadmium substantially the same bond distances as in Tl₁₁⁷⁻.

The trigonal pyramid cluster Tl₅⁷⁻ shown in Figure 3b is C_{3v} in symmetry vs a considerably more distorted C_m type in Na₂K₂₁Tl₁₉⁶ and a similar D_{3h} version in Na₂₃K₉Tl_{15.3}.²⁴ The Tl–Tl bond lengths averaged over each of these clusters are 3.20, 3.22, 3.24 Å, respectively, very close to each other. The

(18) Alvarez, S. *Table of Parameters for Extended Hückel Calculations*; Universitat de Barcelona, June 1989.

(19) Vela, A.; Gázquez, J.-L. *J. Phys. Chem.* **1988**, *92*, 5688.

(20) Sheldrick, G. M. *SHELXS 86*; Universität Göttingen: Germany 1986.

(21) *TEXSAN*, Version 6.0; Molecular Structure Corp.: The Woodlands, TX, 1990.

(22) Walker, N.; Stuart, D. *Acta Crystallogr.* **1983**, *A39*, 158.

(23) Pauling, L. *The Nature of the Chemical Bond*; Cornell University Press: Ithaca, NY, 1960; p 400.

(24) Dong, Z.-C.; Corbett, J. D. *Inorg. Chem.* **1996**, *35*, 3107.

Table 3. Bond and Interatomic Distances in $\text{Na}_9\text{K}_{16}\text{Tl}_{18}\text{Cd}_3$

Tl1-Tl1	3.320(3) × 2	K2-Tl3	4.003(9)	× 3
Tl1-Tl2	3.140(3)	K2-Tl5	4.083(9)	× 2
Tl1-Tl3	3.155(3)	K2-Cd	3.830(4)	× 2
Tl1-K1	3.917(2) × 2	K2-K2	4.09(3)	× 2
Tl1-K1	3.89(1) × 2	K2-K3	4.00(1)	× 2
Tl1-K3	3.98(1) × 2	K2-K4	4.07(1)	× 2
Tl1-Na1	3.19(2)	K2-Na1	4.09(2)	× 4
Tl1-Na2	3.25(2)			
		K3-Tl1	3.98(1)	× 2
Tl2-Tl1	3.140(3) × 3	K3-Tl2	3.73(1)	× 2
Tl2-K3	3.73(1) × 3	K3-Tl3	3.96(1)	× 2
Tl2-Na2	3.335(2) × 3	K3-Tl5	3.691(7)	× 2
		K3-K1	3.96(1)	× 2
Tl3-Tl1	3.155(3) × 3	K3-K2	4.00(1)	× 2
Tl3-K2	4.003(9) × 3	K3-Na1	3.74(1)	× 2
Tl3-K3	3.96(1) × 3	K3-Na2	3.73(1)	× 2
Tl3-Na1	3.30(2) × 3			
		K4-Tl5	3.718(2)	× 6
Tl4-Tl5	3.254(3) × 3	K4-K2	4.07(1)	× 2
Tl4-Cd	3.349(4) × 3			
Tl4-K	3.84(1) × 3	Na1-Tl1	3.19(2)	× 2
Tl4-Na1	3.16(2) × 3	Na1-Tl3	3.30(2)	× 2
		Na1-Tl4	3.16(2)	× 2
		Na1-Tl5	3.36(1)	× 2
Tl5-Tl4	3.254(3)	Na1-Cd	3.07(2)	× 2
Tl5-Tl5	3.136(3)	Na1-K1	3.98(2)	× 2
Tl5-Tl5	5.297(4)	Na1-K2	4.09(2)	× 4
Tl5-Cd	3.115(2) × 2	Na1-K3	3.74(1)	× 2
Tl5-K1	4.08(1)			
Tl5-K2	4.083(9) × 2			
Tl5-K4	3.718(2)	Na2-Tl1	3.225(2)	× 4
Tl5-Na1	3.36(1) × 2	Na2-Tl2	3.335(2)	× 2
		Na2-K1	4.023(8)	× 2
		Na2-K3	3.73(1)	× 2
Cd-Tl4	3.349(4) × 2			
Cd-Tl5	3.115(2) × 4			
Cd-Cd	3.481(8) × 2			
Cd-K2	3.830(4) × 2			
Cd-Na1	3.07(2) × 2			
K1-Tl1	3.917(2) × 2			
K1-Tl1	3.89(1)			
K1-Tl4	3.84(1) × 3			
K1-Tl5	4.08(1)			
K1-K3	3.96(1) × 2			
K1-Na1	3.98(2) × 2			
K1-Na2	4.023(8) × 2			

first vs the last of these distance averages for Tl_5^{7-} are evidently a direct function of the presence of a minority (-1:2) vs a majority (-2:1) of sodium neighbors in the two compounds, respectively. In the present structure, the sodium atoms occur mostly about the higher field Tl_5^{7-} ion, closer but less frequently about the waist, and around the Tl4 vertexes that lie on the 3-fold axis in $\text{Tl}_8\text{Cd}_3^{10-}$. These sodium layers are evident in Figure 1. The distances between the atoms in the polyanions and the cations are pretty normal for alkali-metal-thallium compounds. The shortest K-Tl or K-Cd separations are about 3.73–3.84 Å while the smallest $d(\text{Na-Tl})$ and $d(\text{Na-Cd})$ are 3.07 and 3.16 Å. All of the cations have coordinate numbers of six to Tl and Cd except that only five occur about K2 out to 4.01 Å. Note that a relatively sodium-poor mixture of cations (0.36 at. fraction Na) is necessary to obtain this particular phase from the “soup” that constitutes the precursor alloy melt. (It is clear that clusters persist in the melts.²⁵) The packing and Madelung energy obviously must be optimal at this particular composition. The synthetic advantages of mixed cations have been noted many times before in the isolation of new and novel

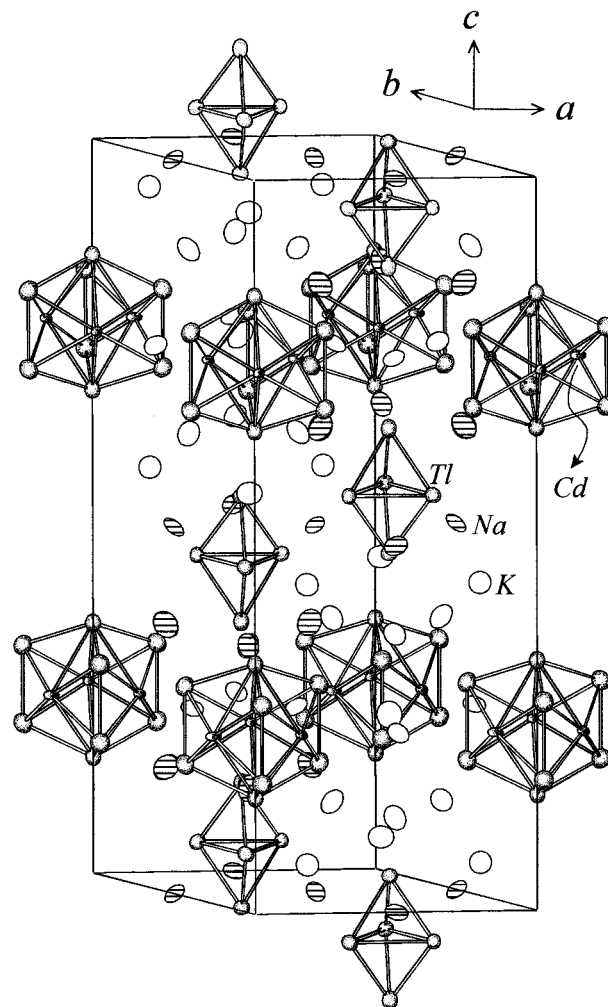


Figure 1. $\sim[110]$ view of the unit cell contents in $\text{Na}_9\text{K}_{16}\text{Tl}_{18}\text{Cd}_3$ (90% probability ellipsoids). The $\text{Tl}_8\text{Cd}_3^{10-}$ clusters lie on horizontal mirror planes at $z = 1/4$, while Tl_5^{7-} units are centered at $z = 0.45, 0.55$, etc.

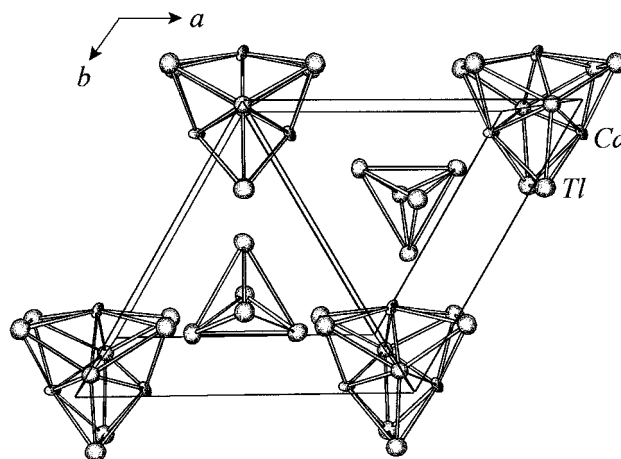


Figure 2. Perspective [001] view of the two cluster layers in $\text{Na}_9\text{K}_{16}\text{Tl}_{18}\text{Cd}_3$.

clusters and compounds.^{3,10,26} Neither variable Na:K proportions or mixed occupancy of cation sites have been noted in any structure during our studies of seven mixed cation thallium phases.

Three distinct cluster compounds are now known in the quaternary Na-K-Cd-Tl systems. The present $\text{Tl}_8\text{Cd}_3^{10-}$

(25) (a) van der Lugt, W. In *Chemistry, Structure and Bonding of Zintl Phases and Ions*; Kauzlarich, S., Ed.; VCH Publishers: New York, 1996; Chapter 4. (b) van der Lugt, W. *J. Phys., Condens. Matter* **1996**, *8*, 6115.

(26) Ganguli, A. K.; Corbett, J. D.; Köckerling, M. *J. Am. Chem. Soc.* **1998**, *120*, 1223.

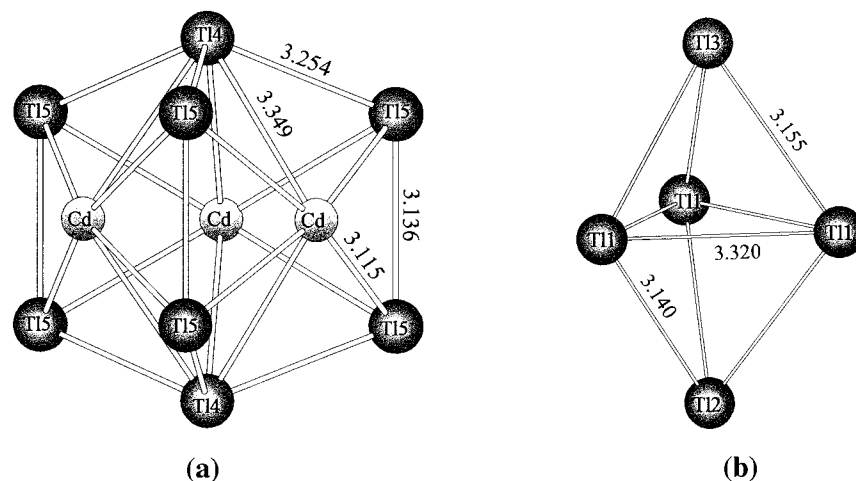


Figure 3. (a) Tl₈Cd₃¹⁰⁻ anions (D_{3h}) with distances ($\sigma \leq 0.003 \text{ \AA}$). (b) the Tl₅⁷⁻ anion (C_{3v}).

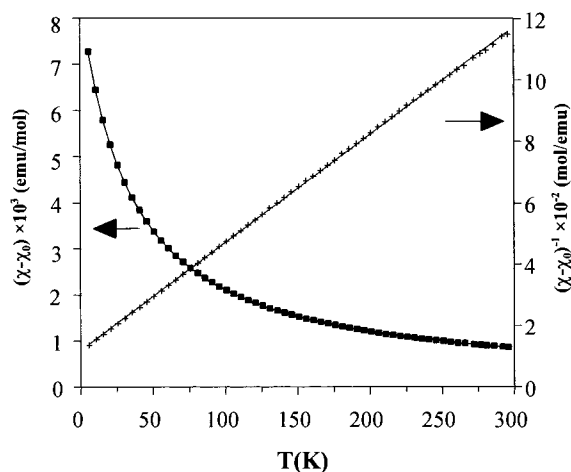


Figure 4. Net molar magnetic susceptibilities ($\chi - \chi_0$) and the inverse as a function of temperature. The solid line is the nonlinear fit to the data (see text).

involves equatorial substitution in the familiar Tl₁₁⁷⁻ unit for the composition Na₉K₁₆Tl₁₈Cd₃, while the other two contain Cd-centered icosahedra Tl₁₂Cd¹²⁻. One, Na₁₄K₆Tl₁₈Cd (which also contains Tl₆⁸⁻) is found at distinctly Na-richer and Cd-poorer compositions,¹² while the other, Na₂K₆Cd₂(Tl₁₂Cd), is Na-poorer and Cd-richer (relative to the thallium content).²⁷ This phase also has some cadmium disordered on sodium sites. Neither of these compounds was recognized during the present study.

Properties and Bonding. High-frequency Q measurements of electrical resistivity of the compound indicate that the title phase is a semiconductor with $\partial\rho/\rho\partial T = -0.32(3)\% \text{ K}^{-1}$ and $\rho_{298} = 210 \mu\Omega\cdot\text{cm}$ (Supporting Information). This is particularly distinctive since many other indium and thallium cluster compounds show moderate metal-like resistivities ($> 200 \mu\Omega\cdot\text{cm}$) even though the phases are diamagnetic and the ions appear to be closed shell.³ The evidently large MO gaps associated with the present cluster anions may be in part responsible for the clear-cut semiconducting characteristics (below), but the odd electron in its formulation (above) must be well-bound as well. Magnetic susceptibility data for Na₉K₁₆Tl₁₈Cd₃ as a function of temperature are shown in Figure 4. Surprisingly, the compound shows a temperature-dependent susceptibility over the entire range, 6–300 K rather than a Pauli-like behavior for

an electron-rich Zintl phase.³ Fitting the data to the nonlinear relationship $(\chi - \chi_0)^{-1} = (T + \theta)/C$ gives the fit shown with $\chi_0 = -1.74(4) \times 10^{-4} \text{ emu mol}^{-1}$, $\theta = -32.8(9) \text{ K}$, $C = 0.2826(6)$, and thence $\mu_{\text{eff}} = 1.504(2) \mu_B$, where χ_0 is a temperature-independent term and θ is the Weiss constant. The observed resistivity and Curie–Weiss magnetic properties indicate a new and novel result, namely, that the one extra electron per formula unit of the title phase, $(\text{Na}^+)_9(\text{K}^+)_{16}(\text{Tl}_5^{7-})_2(\text{Tl}_8\text{Cd}_3^{10-})\text{e}$, is both well localized rather than itinerant and magnetically fairly dilute. In addition, the negative sign of the χ_0 value (above), not the positive value for the common TIP (van Vleck) property, seems to be a nice confirmation of the presence of another effect, the extra diamagnetism associated with the Larmor precession of electron pairs in large cluster orbitals (Langevin terms).²⁸ We have often found it appropriate to correct for this in cluster systems lacking temperature-dependent magnetic properties.^{6–10} The calculated value for the present situation, $-2.1 \times 10^{-4} \text{ emu mol}^{-1}$, is reasonably close to the observed value, $1.74(4) \times 10^{-4} \text{ emu mol}^{-1}$, considering the approximate nature of universal diamagnetic corrections in general.

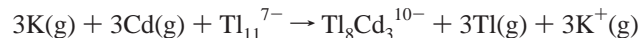
The bonding in Tl₅⁷⁻ and Tl₁₁⁷⁻ type clusters has been described at the EHMO level in previous papers.^{6,8} That in Tl₈Cd₃¹⁰⁻ is naturally quite similar to bonding of the isoelectronic and isosteric cluster Tl₁₁⁷⁻, but their MO intercomparison is otherwise not very informative (Supporting Information). Some energy levels, like 1a', 2a', e', e'', shift to higher energy because of the dominance of the higher lying Cd s and p orbitals therein, and the HOMO–LUMO gap decreases from -2.2 to -1.8 eV . Otherwise, the charge assignment Tl₈Cd₃¹⁰⁻ for the cadmium cluster seems appropriate, with the same $2n - 4$ skeletal electron count as Tl₁₁⁷⁻. This leads to the foregoing description $[(\text{Na}^+)_9(\text{K}^+)_{16}(\text{Tl}_8\text{Cd}_3^{10-})(\text{Tl}_5^{7-})_2 \text{e}^-]$ in which the apparent charges should be recognized as only oxidation state distributions. With the relatively large gaps in the MO descriptions of both clusters, we presume the extra electron is somehow trapped in a cavity defined by the alkali-metal cations (or in an extended, isolated cluster state), analogous to that giving Curie–Weiss behavior in the recently discovered $(\text{Cs}^+)_8(\text{Ga}_{11}^{7-})\text{e}^-$,⁴ but no evidence is at hand on how or where. Localization of this electron in the LUMO of either cluster would be expected to produce an appreciable axial elongation, which is not seen.

The relative energetics of these elements and clusters can be approached another way in terms of the exchange (and reduc-

(27) Tillard-Charbonnel, M. M.; Belin, C. H.; Manteghetti, A.; Flot, D. *M. Inorg. Chem.* **1996**, *35*, 2583.

(28) Sevov, S. C.; Corbett, J. D. *Inorg. Chem.* **1992**, *31*, 1895.

tion) reaction



The appropriate sum of the ionization energy of potassium and of the orbital energies of the exchanged elements and the two clusters alone is energetically neutral (+3 kJ), and this becomes only +61 kJ when the three metals are put in their standard (solid) states via the appropriate sublimation energies.²⁹ The metal exchange to produce the more noble thallium is an appreciable factor here, almost twice the difference in orbital energies of the two clusters. There must also be an increase in Madelung energy for the above process in the solid state. We have not attempted to include this, but it should certainly make the real process more favorable than approximated here.

The substitution of Cd for the waist capping atoms in Tl_{11}^{7-} is interesting in relationship to the generally well-established trends in this type of reaction elsewhere in chemistry, that substitution tends to take place at those positions that generate a more uniform charge distribution.^{30,31} The Mulliken charges within Tl_{11}^{7-} and $\text{Tl}_8\text{Cd}_3^{10-}$ were calculated on the basis of the EHMO scheme with the $\text{Tl}_8\text{Cd}_3^{10-}$ (D_{3h}) structural model for both. The three types of atoms in Tl_{11}^{7-} were found to have

charges of -0.65 on the axial sites (Tl4), -0.26 on the waist-capping atoms on the σ_h plane (vice Cd), and -0.82 on the prismatic positions. Consequently, the more negative Cd atoms ($\text{Cd}^- \cong \text{Tl}^0$, etc.) properly substitute on the waist position to produce a new charge distribution of -0.80 (Tl4), -0.70 (Cd), and -1.05 (Tl5). This traditional substitution direction contrasts with what was deduced years ago as a nontraditional Tl substitution in the clusters in a mixed cluster site in $(2,2,2\text{-crypt K}^+)_3(\text{TlSn}_8^{3-} \cdot \text{TlSn}_9^{3-})_2$. In each case, the earlier Tl element had substituted in the lower order, higher charged capping site in the hypothetical Sn_9^{2-} (D_{3h}) (face-capping) and Sn_{10}^{2-} (D_{4d}) (axial).³² The Madelung part of the crystal energy is clearly much less in phases of this type. Nonetheless, we will shortly report on the novel, and modestly contradictory, substitution of Cd on both axial positions instead (Tl4, Figure 3a) to give $\text{Tl}_9\text{Cd}_2^{7-}$ in a salt with only potassium cations.¹⁶ In this case, a concomitant axial compression leads to a good transannular Cd–Cd bond, analogous to that found within $\text{Tl}_9\text{Au}_2^{9-}$ in $\text{K}_{18}\text{Tl}_{20}\text{Au}_3$.¹⁴

Acknowledgment. The authors thank J. Ostenson for the magnetic susceptibility data and W. Straszheim for the EDS measurements.

Supporting Information Available: Tables of additional data collection and refinement parameters and anisotropic displacement parameters, and figures of the resistivity data and MO results (4 pages). Ordering information is given on any current masthead page.

IC9807792

(29) Greenwood, N. N.; Earnshaw, A. *Chemistry of the Elements*, 2nd ed.; Butterworth-Heinemann: Oxford, 1997.

(30) Gimarc, B. M.; Ott, J. J. *J. Am. Chem. Soc.* **1986**, *108*, 4298.

(31) Hall, M. B.; Fenske, R. F. *Inorg. Chem.* **1972**, *11*, 768.

(32) Burns, R. C.; Corbett, J. D. *J. Am. Chem. Soc.* **1982**, *104*, 2804.